10-15-1998

Luminescence Properties of Thin Film Ta2 Zn3 O8 and Mn Doped Ta2 Zn3 O8

Philip D. Rack
Advanced Vision Technologies, Inc.

Michael D. Potter
Advanced Vision Technologies, Inc.

Santosh Kurinec
Rochester Institute of Technology

Wounjhang Park
Georgia Institute of Technology

John Penczek
Georgia Institute of Technology

See next page for additional authors

Recommended Citation
P.D. Rack, M.D. Potter, S. Kurinec, W. Park, J. Penczek, B.K. Wagner, and C.J. Summers, Journal of Applied Physics 84, 4466 (1998). https://doi.org/10.1063/1.368672

Luminescence properties of thin film $Ta_2Zn_3O_8$ and Mn doped $Ta_2Zn_3O_8$

Philip D. Rack[a] and Michael D. Potter
Advanced Vision Technologies, Inc., 150 Lucius Gordon Drive, Suite 215, West Henrietta, New York 14586

Santosh Kurinec
Microelectronic Engineering, Rochester Institute of Technology, Rochester, New York 14623

Wounjhang Park, John Penczek, Brent K. Wagner, and Christopher J. Summers
Phosphor Technology Center of Excellence, Georgia Institute of Technology, Atlanta, Georgia 30332

(Received 13 April 1998; accepted for publication 7 July 1998)

Blue luminescence from $Ta_2Zn_3O_8$ and green luminescence from Mn doped $Ta_2Zn_3O_8$ has been observed under low voltage cathodoluminescent excitation. In this article, the luminescence mechanisms of $Ta_2Zn_3O_8$ and Mn doped $Ta_2Zn_3O_8$ are discussed in detail. The results suggest that the intrinsic blue luminescence of $Ta_2Zn_3O_8$ results from a metal-to-ligand transition, whereas the green luminescence of Mn doped $Ta_2Zn_3O_8$ results from the Mn $^4T_1-^6A_1$ transition. The suppression of the blue intrinsic luminescence in Mn doped $Ta_2Zn_3O_8$ suggests that efficient energy transfer from the host material to the Mn occurs. This energy transfer phenomenon is also discussed by comparing the photoluminescence excitation spectra of both thin film materials. Finally, the relative efficiency versus voltage and current density is demonstrated and discussed pertaining to field emission device operation.

I. INTRODUCTION

Flat panel display technologies such as field emission displays (FED) and vacuum fluorescent displays (VFDs) have rekindled a significant interest in low voltage cathodoluminescent materials. While many efficient sulfide based phosphors have been explored as possible low voltage phosphors, the volatility of sulfur has prohibited their use in FEDs or VFDs. There are basically two deleterious effects that sulfide based phosphors have on these devices. First of all, electron stimulated reactions have been shown to form a sulfur deficient nonluminescent layer on the phosphor surface, which degrades the phosphor efficiency.[1] Second, the electron stimulated reaction by-products are known to poison the electron emitters.

The two most studied low voltage cathodoluminescent phosphors are ZnO and $ZnGa_2O_4$. Both have reasonable conductivity, which inhibits phosphor charging at low voltages. While ZnO is very efficient at low voltages, its chromaticity lies in the blue-green region. $ZnGa_2O_4$ is not as efficient as ZnO, but depending on the Zn/Ga ratio, it can have good blue color saturation.[2,3] Furthermore, $ZnGa_2O_4$ has been doped with Mn^{+2}, which results in a well-saturated green luminescence.[3–5]

More recently, blue luminescence in thin film[6] and powder[7] $Ta_2Zn_3O_8$ has been reported under low voltage cathodoluminescent excitation. The spinel crystal structure was described, and a threshold voltage of 10 V and CIE coordinates of $x=0.160$ and $y=0.075$ were reported. In this article, we discuss the luminescence mechanisms of $Ta_2Zn_3O_8$ and Mn doped $Ta_2Zn_3O_8$, and also examine its relative intensity and efficiency as a function of voltage and current density.

II. EXPERIMENTAL PROCEDURE

The $Ta_2Zn_3O_8$ thin films were made by sputtering a layer of ZnO (99.999%) and Ta (99.999%) and annealing this bilayer structure at 1100 °C in a nitrogen ambient. For the Mn-doped $Ta_2Zn_3O_8$ thin films, a thin layer of Mn (~5 nm) was sputtered on top of $Ta_2Zn_3O_8$ thin film and reannealed at 1100 °C to drive in the Mn. A Perkin Elmer 2400 sputter system was used and the sputtering conditions were 7 mTorr Ar and rf sputtering powers ranging from 500 to 700 W. Low voltage cathodoluminescence (CL) spectra were measured with a Plasma Scan PSS-2 spectrometer, and CL intensity measurements were taken with an International Light 1700 photometer equipped with a photopic filter. Photoluminescence measurements were performed by using the 275 nm output of an Ar ion laser. The tunable light source for photoluminescence (PL) excitation measurements was provided by a 450 W Xe lamp coupled with a Spex monochrometer. The luminescence signal was dispersed by a Spex 1000 M monochrometer and detected by a thermoelectrically cooled GaAs photomultiplier tube (PMT).

III. RESULTS

Figure 1 shows the cathodoluminescence emission spectrum (UV filtered and unfiltered), and the photoluminescence excitation spectrum (monitored at $\lambda=385$ nm) of $Ta_2Zn_3O_8$. The unfiltered emission spectrum has a peak wavelength of ~385 nm, whereas the filtered spectrum has a peak wavelength of ~420 nm. The luminescence decay measurement of the $Ta_2Zn_3O_8$ material is shown in Fig. 2 which has a decay time of 1.13 μs (to $1/e$). Figure 3 shows the thin film

[a]Electronic mail: pdrdav@rit.edu

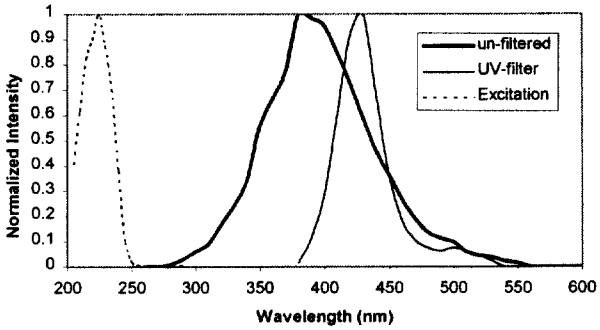

FIG. 1. Unfiltered and a UV filtered cathodoluminescence emission spectrum and photoluminescence excitation spectrum of a $Ta_2Zn_3O_8$ thin film.

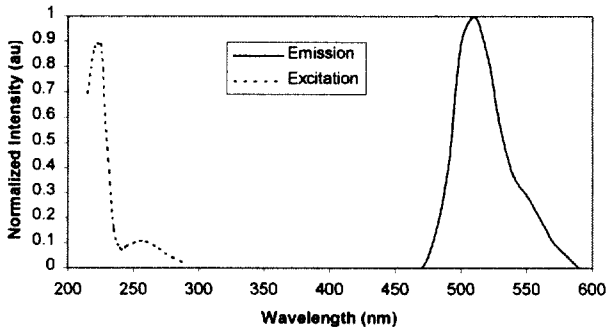

FIG. 3. Cathodoluminescence emission spectrum and photoluminescence excitation spectrum of a Mn doped $Ta_2Zn_3O_8$ thin film.

Mn-doped $Ta_2Zn_3O_8$ CL emission spectrum and the corresponding PL excitation spectrum (monitored at $\lambda = 514$ nm). The green emission spectrum of the Mn-doped $Ta_2Zn_3O_8$ has a peak wavelength of ~514 nm.

Figure 4 shows the normalized CL intensity (a) and efficiency (b) as a function of voltage (at 10 μA) of the $Ta_2Zn_3O_8$ and the Mn-doped $Ta_2Zn_3O_8$. The intensity and efficiency increase linearly for both phosphors in the measured voltage range of 300–1000 V. Figure 5 shows $Ta_2Zn_3O_8$ and the Mn-doped $Ta_2Zn_3O_8$ CL intensity (a) and efficiency (b) as a function of current density (at 1000 V). While the intensity of both phosphors continues to increase at current densities up to 100 $\mu A/cm^2$, the efficiencies of each material begin to saturate below 10 $\mu A/cm^2$.

IV. DISCUSSION

A. Thin film properties

One problem with thin film phosphors for display applications has been internal reflection. Internal reflection causes a majority (up to 90%) of the light generated in the phosphor layer to be "piped" along the horizontal direction and essentially lost. In $Ta_2Zn_3O_8$ thin films, there is no apparent "light piping," which is attributed to the columnar grain structure. These fine columnar grains of ~100 nm diameter are much smaller than the wavelength of the emitted light. Subsequently, the grain boundaries effectively scatter (via Rayleigh scattering) light rather than internally reflecting the light in the horizontal direction. Because the Mn concentrations are less than 1 mol %, the Mn doped $Ta_2Zn_3O_8$ microstructure is similar to the pure $Ta_2Zn_3O_8$ films and similar scattering phenomenon occur.

Similar to ZnO and $ZnGa_2O_4$, thin film $Ta_2Zn_3O_8$ has a low resistivity. A low resistivity is important because it prevents the phosphor from charging at low voltages. $Ta_2Zn_3O_8$ resistivities of 50 $\mu\Omega$ cm were measured using four point probe measurements of a $Si/SiO_2/Ta_2Zn_3O_8$ thin film stack. While the exact conduction mechanism of $Ta_2Zn_3O_8$ is not fully understood, there are two possible mechanisms that make $Ta_2Zn_3O_8$ conducting. First of all, a high concentration of oxygen vacancies could result in a shallow donor level that thermally populates the conduction band at room temperatures. Second, a second phase of oxygen deficient ZnO could be intermixed with $Ta_2Zn_3O_8$ which is known to be a good transparent conductor. Current studies are underway to determine the exact conduction mechanism responsible in $Ta_2Zn_3O_8$.

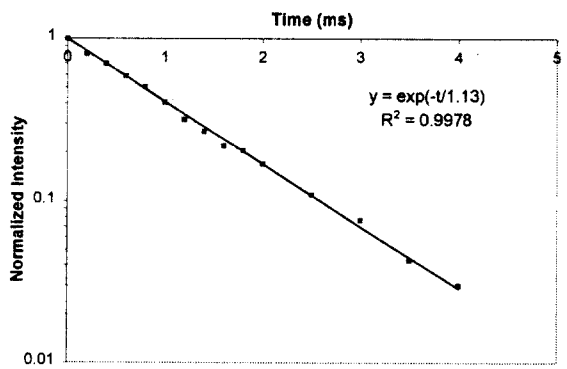

FIG. 2. Luminescence decay plot of the Ta–O_6 emission ($\lambda = 385$ nm).

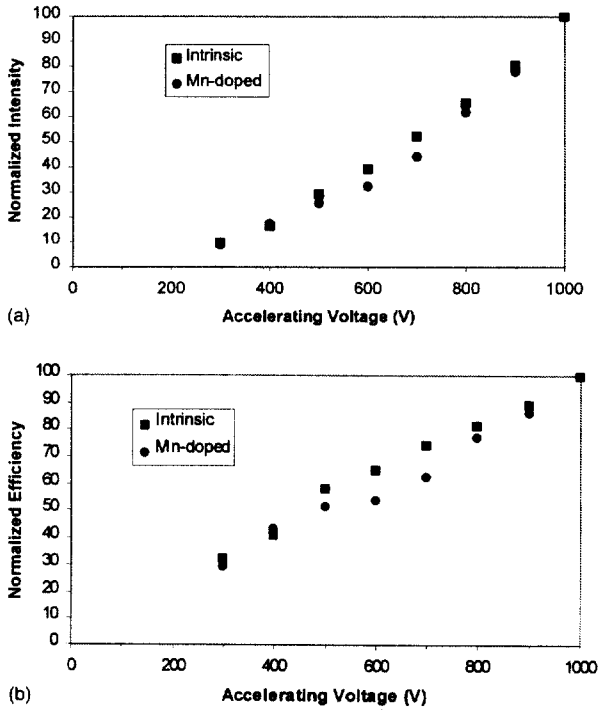

FIG. 4. Cathodoluminescence intensity (a) and efficiency (b) vs. voltage for a $Ta_2Zn_3O_8$ and a Mn doped thin film (constant current).

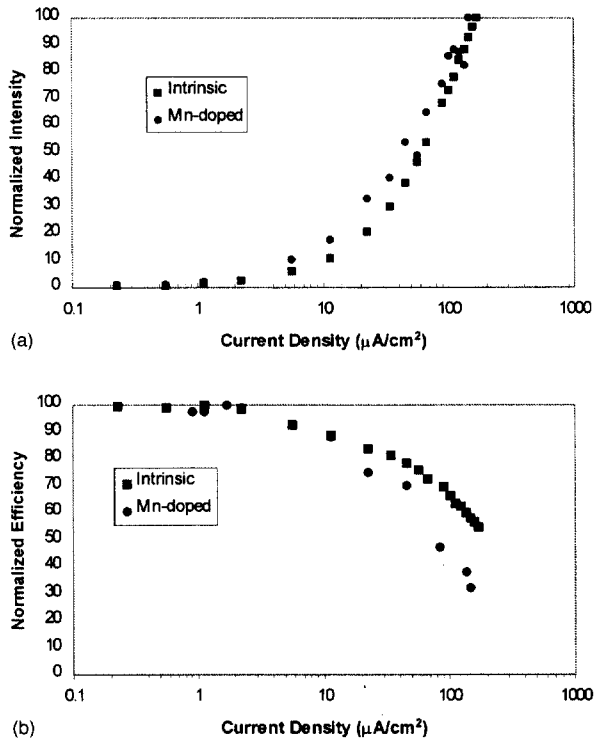

FIG. 5. Cathodoluminescence intensity (a) and efficiency (b) vs. current density for a $Ta_2Zn_3O_8$ and a Mn doped thin film (constant voltage).

B. $Ta_2Zn_3O_8$ luminescence

Figure 1 shows the unfiltered and ultraviolet (UV) filtered low voltage CL emission spectra of $Ta_2Zn_3O_8$. The unfiltered, $Ta_2Zn_3O_8$ has broadband emission with a peak wavelength of ~385 nm, while the filtered spectrum has a peak at ~420 nm. While a significant portion of the broadband emission occurs in the UV, efficient blue luminescence is observed through an attenuating UV filter.

The radiative transition responsible for the high-energy luminescence in $Ta_2Zn_3O_8$ is a metal-to-ligand radiative transition, where tantalum is the metal and oxygen is the ligand. More specifically, the excited state is the $5d^0$ state of the tantalum metal whereas the ground state is the $2p^6$ state associated with the oxygen ligand. As reported earlier, $Ta_2Zn_3O_8$ has a spinel crystal structure, which has interpenetrating octahedral Ta sites and tetrahedral Zn sites with oxygen as the common anion. Octahedrally coordinated $(TaO_6)^{-7}$ and other octahedrally coordinated transition metals (i.e., MoO_6 WO_6, TiO_6) are known to luminesce rather efficiently via this metal-to-ligand transition.[8]

Because this type of transition occurs between a bonding state ($O-2p^6$), and an antibonding state ($Ta-5d^0$), there is significant reorganization in the electronic structure upon excitation. Subsequently, a large Stokes shift between the excitation spectrum and the emission spectrum results. Figure 1 shows the excitation and emission spectrum of $Ta_2Zn_3O_8$ phosphor, which exhibits a Stokes shift of ~21 000 cm^{-1} (2.6 eV).

This large Stokes shift is critical to luminescent materials like $Ta_2Zn_3O_8$ which have an activator concentration of essentially 100%. Typically, energy transfer probabilities increase at higher activator concentrations, which quench luminescence in many materials. In general, there are two types of energy transfer: (1) radiative transfer whereby the sensitizer emits a photon and the activator subsequently absorbs the photon; and (2) nonradiative transfer associated with resonance between the sensitizer and the activator.[9] Radiative transfer between a sensitizer and activator depends largely on the fluorescence efficiency of the activator at the specific wavelength of the sensitizer emission. For nonradiative transfer, two mechanisms are important, namely energy transfer due to exchange interactions, and energy transfer via electric or magnetic multipolar interactions. The probability (P_{SA1}) of energy transfer due to exchange interactions is given by

$$P_{SA1} \propto f_{SA} E_{SA}, \tag{1}$$

where f_{SA} is a function of the wavefunction overlap between the sensitizer and the activator [and consequently $\propto \exp(-R_{SA})$, where R_{SA} is the distance between the sensitizer and the activator], and E_{SA} is the energy overlap between the sensitizer emission and the activator absorption.

The probability (P_{SA2}) of energy transfer due to a multipolar interaction is given by

$$P_{SA2} \propto \frac{Q_{SA} E_{SA}}{\tau_s R_{SA}^n} = g_{SA} E_{SA}, \tag{2}$$

where Q_A is the absorption band area of the activator, and τ_S is the radiative decay time of the sensitizer. The power n is 6 for dipole–dipole interactions, and 8 for dipole–quadrapole interactions.

From these expressions, the two parameters that are important for both types of energy transfer is the spectral overlap of the sensitizer emission and activator absorption (E_{SA}), and the distance between sensitizer and activator (R_{SA}). In the undoped $Ta_2Zn_3O_8$ material, S and A are the same and energy transfer between $Ta-O_6-Ta-O_6$ sites must be considered. Because there is essentially 100% activator concentration in $Ta_2Zn_3O_8$ the distance between activator sites is relatively short which would promote energy transfer. However, because of the large Stokes shift there is no appreciable overlap between the emission and excitation spectra of $Ta_2Zn_3O_8$. Consequently, energy transfer is suppressed and efficient radiative recombination occurs.

Figure 4 shows the $Ta_2Zn_3O_8$ CL intensity (a) and efficiency (b) as a function of voltage (at constant current) and Fig. 5 shows the CL intensity (a) and efficiency (b) as a function of current density (at constant voltage). Figure 4 shows that the intensity and efficiency continue to increase as a function of increasing voltage in the range of 300–1000 V. This is expected because the penetration depth and excitation volume increases with increasing voltage. Figure 5 shows that while the intensity of the $Ta_2Zn_3O_8$ phosphor continues to increase as a function of increasing current density, the efficiency saturates at high current densities. Though $Ta_2Zn_3O_8$ does exhibit some current saturation at high current densities, its relative efficiency of 67% at 100 $\mu A/cm^2$ is better than most phosphor materials.

The current saturation properties are particularly important to low voltage display applications because higher cur-

rent densities are used to offset the lower voltages. There are basically two major contributions to current saturation in phosphor materials. One contribution is activator ground state depletion, and the second contribution is thermal quenching. Ground state depletion is a regime in which all of the activators in the excitation volume are in the excited state. Yang *et al.*[10] have investigated activator ground state depletion in detail and have shown that ground state depletion is directly proportional to the luminescence decay time. They concluded that phosphors with shorter decay times are more resistant to current saturation because of activator recycling. The CL luminescence decay plot of $Ta_2Zn_3O_8$ is shown in Fig. 2, which has a decay time to $1/e(\tau_e)$ of 1.13 μs. This is a relatively short decay time, which is in agreement with the good current saturation behavior.

The thermal quenching contribution to current saturation occurs because the nonradiative recombination process is thermally stimulated. Therefore at higher current densities, where Joule heating is more severe, the nonradiative recombination rate increases. While it is rather difficult to distinguish between these two contributions to current saturation, we believe both are contributing to the current saturation observed in $Ta_2Zn_3O_8$.

C. Mn doped $Ta_2Zn_3O_8$ luminescence

Figure 3 shows the CL emission spectrum for the Mn doped $Ta_2Zn_3O_8$ thin film which has a peak maximum at 514 nm and CIE coordinates of $x=0.14$ and $y=0.714$. In the $Ta_2Zn_3O_8$ spinel structure, the Mn ions likely substitute for Zn^{+2} sites which would suggest the Mn ion has a +2 oxidation state. While Mn can occur as +2, +3, +4, and +5 ions in some materials, because Zn^{+2} and Mn^{+2} have similar ionic radii (Mn=0.08 nm, and Zn=0.074 nm,) in several Zn-based phosphors Mn occupies a Zn^{+2} site. Chemical state analysis of the Mn oxidation state in the $Ta_2Zn_3O_8$ is currently under investigation. Assuming Mn substitutes for Zn, this suggests that the Mn^{+2} luminescent center has a tetrahedral crystal field which relaxes the parity selection rule because of the lack of inversion symmetry.

Figure 3 shows that under CL excitation, the host emission is completely suppressed in the Mn doped film, and only the $^4T_1-^6A_1$ transition of Mn emits efficiently. This observation suggests that the $Ta_2Zn_3O_8$ host efficiently transfers its energy to the Mn luminescent center. To elucidate the energy transfer phenomenon, Fig. 3 also shows the PL excitation spectrum of the Mn doped $Ta_2Zn_3O_8$ thin film. The Mn doped $Ta_2Zn_3O_8$ PL excitation spectrum has two main peaks, one at ~255 nm and one at ~220 nm. The 255 nm peak is attributed to the O–Mn charge transfer excitation which occurs from direct excitation from the oxygen ligand to the manganese excited state. The second peak at ~220 nm is similar in energy and shape to the undoped $Ta_2Zn_3O_8$ excitation, and is therefore attributed to host excitation. The magnitude of the host lattice excitation for the Mn doped $Ta_2Zn_3O_8$ confirms that efficient energy transfer from the host lattice to the Mn luminescent center is occurring.

While radiative energy transfer is not suspected to occur due to the low oscillator strength of the Mn, nonradiative energy transfer is suspected to occur. From expression (1) and (2), efficient energy transfer via exchange interactions or multipole interactions requires both a short sensitizer ($Ta-O_6$) to activator (Mn) distance, and appreciable spectral overlap between the sensitizer emission and the activator absorption. Because Mn^{+2} occupies tetrahedral Zn^{+2} sites, the sensitizer-to-activator distance (R_{SA}) is short as it is simply the nearest neighbor Ta cation site. From Figs. 1 and 3, there is a small spectral overlap between the $Ta_2Zn_3O_8$ host emission and the Mn charge transfer excitation band. According to Blasse and Bril,[11] because the sensitizer emission band overlaps with an allowed absorption transition of the activator (i.e., O–Mn), the energy transfer is probably dominated by electric multipole interactions. Conversely, if the sensitizer emission band overlaps forbidden activator transitions, energy transfer via exchange interactions dominate.

Figure 4 also shows the Mn doped $Ta_2Zn_3O_8$ CL intensity (a) and efficiency (b) as a function of voltage (at constant current) and Fig. 5 shows the CL intensity (a) and efficiency (b) as a function of current density (at constant voltage). Figure 4 again reveals that the intensity and efficiency increases as a function of increasing voltage. This is again consistent with a deeper penetration depth and a larger excitation volume at higher voltages. Similar to $Ta_2Zn_3O_8$, Fig. 5 shows that the Mn doped $Ta_2Zn_3O_8$ intensity increases as a function of increasing current density, and the efficiency saturates at higher current densities. Compared to the undoped $Ta_2Zn_3O_8$ the Mn doped $Ta_2Zn_3O_8$ saturates more severely at higher current densities (45% at 100 $\mu A/cm^2$).

The more severe current saturation of Mn doped $Ta_2Zn_3O_8$ is most likely due to ground state depletion of Mn luminescent centers. While luminescent decay measurements were not performed on the Mn doped, $Ta_2Zn_3O_8$, the Mn decay constant is relatively long because it is both spin and parity forbidden (though parity rule is relaxed for the tetrahedral field). For instance, in $ZnGa_2O_4$, the Mn^{+2} decay rate has been measured and ranges from 4 to 10 ms.[3] Taking the ratio of the decay rates of the Mn emission and the $Ta_2Zn_3O_8$ emission (~1000) reveals that for a given time interval, the $Ta-O_6$ centers "recycle" 1000 times more than the Mn centers. This translates into better resistance to ground state depletion for the $Ta-O_6$ centers. Though ground state depletion is believed to dominate the current saturation behavior for the Mn doped $Ta_2Zn_3O_8$ material, thermal quenching effects also contribute. In particular, beam induced heating in the Mn doped $Ta_2Zn_3O_8$ material can stimulate energy migration along Mn sites to killer centers.

V. CONCLUSIONS

Blue luminescence from intrinsic $Ta_2Zn_3O_8$ and green luminescence from Mn doped $Ta_2Zn_3O_8$ has been observed under low voltage cathodoluminescent excitation. The intrinsic blue luminescence of the $Ta_2Zn_3O_8$ results from a Ta $5d^0-O\ 2p^6$ metal-to-ligand transition ($Ta-O_6$ octahedral symmetry), whereas the green luminescence of the Mn doped $Ta_2Zn_3O_8$ results from the Mn $^4T_1-^6A_1$ transition (Mn^{+2} tetrahedral symmetry). In both thin film phosphors, the cathodoluminescence intensity and efficiency increase

linearly with excitation voltage which is due to deeper electron penetration at higher voltages. In addition, the cathodoluminescence intensity increases with increasing current density in both materials, however the cathodoluminescence efficiencies saturate at higher current densities. At 100 $\mu A/cm^2$ the relative efficiency of $Ta_2Zn_3O_8$ is 67%, whereas the relative efficiency of the Mn doped $Ta_2Zn_3O_8$ is 45%. The more severe current saturation in the Mn doped $Ta_2Zn_3O_8$ is attributed to ground state depletion because of the slow luminescence decay rate of the Mn(4–10 ms) versus the Ta–O_6 (1.13 μs).

ACKNOWLEDGMENTS

P.D.R., M.D.P., and S.K. would like to acknowledge the support of NSF through an STTR Grant No. DMI-9712200, and W.P., J.P., B.K.W., and C.J.S. would like to acknowledge the support of the Phosphor Technology Center of Excellence (DARPA Grant No. MDA972-93-1-003).

[1] P. H. Holloway, J. Sebastian, T. Trottier, and H. Swart, Solid State Technol. **38**, 47 (1995).
[2] S. Itoh, H. Toki, Y. Sato, K. Morimoto, and T. Kishino, J. Electrochem. Soc. **138**, 1509 (1995).
[3] S. H. M. Poort, D. Cetin, A. Meijerink, and G. Blasse, J. Electrochem. Soc. **144**, 2179 (1997).
[4] L. E. Shea, R. K. Datta, and J. J. Brown, Jr., J. Electrochem. Soc. **141**, 1950 (1994).
[5] T. K. Tran, W. Park, J. W. Tomm, B. K. Wagner, S. M. Jacobsen, C. J. Summers, P. N. Yocom, and S. K. McClelland, J. Appl. Phys. **78**, 5691 (1995).
[6] R. J. Langley, G. F. Pettis, S. K. Kurinec, and M. D. Potter, Proceedings of the Second International Conference on the Science and Technology of Display Phosphors, November 1996, San Diego, CA (1996), p. 39.
[7] S. K. Kurinec and M. D. Potter, SID Digest, May 1997, Boston, MA (1997), Vol. XXVIII, p. 1077.
[8] G. Blasse, *Structure and Bonding* (Springer, Heidelberg, 1980), Vol. 42, pp. 1–42.
[9] R. C. Powell and G. Blasse, *Structure and Bonding* (Springer, Heidelberg, 1980), Vol. 42, pp. 43–96.
[10] S. Yang, F.-L. Zhang, S. M. Jacobsen, C. J. Summers, P. N. Yocom, and S. McClelland, Proc. SPIE **2408**, 194 (1995).
[11] G. Blasse and A. Bril, J. Chem. Phys. **47**, 1920 (1967).